

Article

Assessment of Community Vulnerability to Different Types of Urban Floods: A Case for Lishui City, China

Quntao Yang ^{1,2} , Shuliang Zhang ^{1,2,*}, Qiang Dai ^{1,2} and Rui Yao ^{1,2}

¹ School of geography, Nanjing Normal University, Nanjing 210023, China; yang_1990@outlook.com (Q.Y.); q.dai@bristol.ac.uk (Q.D.); yaorui1226@163.com (R.Y.)

² Key Laboratory of VGE of Ministry of Education, Nanjing 210023, China

* Correspondence: zhangshuliang@njnu.edu.cn

Received: 6 August 2020; Accepted: 21 September 2020; Published: 23 September 2020



Abstract: Urban flooding is a severe and pervasive hazard caused by climate change, urbanization, and limitations of municipal drainage systems. Cities face risks from different types of floods, depending on various geographical, environmental, and hydrometeorological conditions. In response to the growing threat of urban flooding, a better understanding of urban flood vulnerability is needed. In this study, a comprehensive method was developed to evaluate the vulnerability of different types of urban floods. First, a coupled urban flood model was built to obtain the extent of influence of various flood scenarios caused by rainfall and river levee overtopping. Second, an assessment framework for urban flood vulnerability based on an indicator method was used to evaluate the vulnerability in different flood hazard scenarios. Finally, the method was applied to Lishui City, China, and the distribution and pattern of urban flood vulnerability were studied. The results highlight the spatial variability of flooding and the vulnerability distributions of different types of urban floods. Compound floods were identified to cause more severe effects in the urban areas.

Keywords: urban flood; vulnerability; community; fluvial flood; pluvial flood; compound flooding

1. Introduction

Floods, which can cause widespread social and economic damage and even threaten human life, are one of the most severe and frequent natural hazards in urban areas [1,2]. Under rapid urbanization and climate change, the effects of the flooding are becoming worse in urban areas [2–4]. Reducing the effects of urban flooding on communities has become an essential requirement in urban disaster management [5,6]. Many cities and communities have tried to mitigate the effects of urban flooding through structural measures (e.g., increasing urban drainage capacity and building dams) and non-structural measures (e.g., enhancing flood risk awareness) [7–9]. Both approaches rely on the knowledge and resources of multiple sectors and communities in terms of risk reduction strategies, experiences, and lessons; knowledge sharing can be especially valuable among communities with similar vulnerability characteristics [10]. Therefore, vulnerability assessment has become an essential tool for communities to cope with the adverse effects of urban flooding.

Urban communities in complex hydrometeorological environments can face multiple threats from various types of flood, such as urban pluvial floods and fluvial floods [11]. Many studies have considered the risks and vulnerabilities of urban flooding; these research works have primarily focused on fluvial floods, which are considered to result in severe consequences. However, the impacts of other types of floods can be comparable to those of fluvial floods, such as pluvial flooding when rainfall reaches a certain level [12]. Different types of urban flooding are gradually being given more attention. Furthermore, flood risk and vulnerability for different types of floods have been addressed in several studies [13,14]; however, in each study, the different types of floods were considered

separately and on a comparative basis. Furthermore, though several studies have considered the hazards associated with different types of flood using flood modeling and geographic information systems (GIS), they have ignored social and economic factors [15–17]. The risk and vulnerability of compound flooding, which is caused by multiple flood factors, have not been considered. In the context of global change, the intensification of extreme meteorological and hydrological events has led to an increase in compound events, especially compound flooding [18–20]; therefore, there is an urgent need for multiple types of floods to be considered in the vulnerability analysis of urban flooding.

Vulnerability is composed of exposure, sensitivity, and adaptive capacity, especially in the field of disaster risk management [13,21–23]. At present, research on urban flood vulnerability has focused on the vulnerability curve method and indicator-based methods. The vulnerability curve, also called the vulnerability function, represents the relationship between the hazard of disasters and the losses of the receptor, and is always used in physical vulnerability assessment. The assessment of integrated vulnerability and the physical, social, and economic dimensions considered always use indicator-based methods instead of the vulnerability curve, which cannot express many intangible social effects induced by a disaster. The widely used indicator-based method has strong operability for various spatial scales and research objects. Moreover, the method is simple to apply and mainly includes the selection of indicators based on the research object and data to construct the index system, as well as the determination of indicator weights and the resulting integrated vulnerability index [24,25].

Considering the differences in local physical, social, and economic conditions, vulnerability may vary in different communities. Therefore, “place-based” vulnerability is widely accepted [3,21]; abundant geospatial data are usually required for vulnerability assessment, or the original structured data may be converted into geospatial data. GIS methods, which specialize in processing geospatial data, are widely used in various risk and vulnerability assessments [26–28]. Meanwhile, detailed disaster information, which cannot be met by simple disaster record data, is also needed for disaster-specific vulnerability assessment. For flood vulnerability assessment, the flood hazard must be given priority. Currently, flood modeling is increasingly applied to various flood risk and vulnerability studies to obtain more detailed flood information [29,30]. The complete process of a flood can be expressed through a flood model, which is a suitable and frequently used technique to compensate for the shortcomings of actual observational data. However, flood modeling is made more challenging by the complex drainage environments in urban areas. Generally, urban drainage processes are more complex than natural watersheds, and include surface and sewer network runoff, many artificial facilities for rainwater management, and complex terrain. Therefore, flood simulations in urban areas require specialized models. Many hydrological and hydrodynamic models are available for urban flood modeling (e.g., MIKE URBAN, Sobek urban, Infoworks ICM, XPSWMM, and PCSWMM); however, most are commercial models or software, for which copyrights and costly prices limit their use in academic research. Fortunately, several open-source models and free software can provide similar functions (e.g., 1D modeling in a stormwater management model (SWMM) and 2D modeling in LISFLOOD-FP) [31–33]. Therefore, GIS and flood modeling have become essential tools and methods in urban flood vulnerability studies.

The motivation for this study was as follows. First, different types of urban floods, including pluvial floods, fluvial floods, and compound floods under combined river levee overtopping and rainstorms, were simulated to obtain the extent of urban flooding in different disaster scenarios. A 1D–2D coupled urban flood model based on open-source models was built for flood modeling. This model can simulate urban drainage network runoff and urban surface runoff to reflect urban drainage processes. The analytic hierarchy process (AHP) method was used to evaluate flood exposure, sensitivity, and adaptive capacity by combining flood modeling with spatial, physical, and socioeconomic data on urban community scales. Point of interest (POI) data, which can expand the data source and take advantage of GIS technology for multi-source data fusion, were selected together with socioeconomic data to conduct vulnerability research, obtain more adequate indicators, and fully use the geospatial data. Finally, an integrated flood vulnerability index composed of exposure,

sensitivity, and adaptive capacity was built using the weighted linear combination (WLC) method. Lishui City, China was selected for a case study for scenario analyses.

2. Materials and Methods

2.1. Study Area

The Liandu District, the main urban area of Lishui City, China, was selected as the study area. Lishui City is located in southeast Zhejiang Province. Liandu District is a unique municipal district, and 25 communities were selected for analysis (Figure 1). The community, like a village, is the smallest administrative and demographic unit in China and is divided by local administrators. The study area covered approximately 45 km² and is characterized by low-lying topography with hills and mountains to the north and west and the Oujiang River to the south and east.

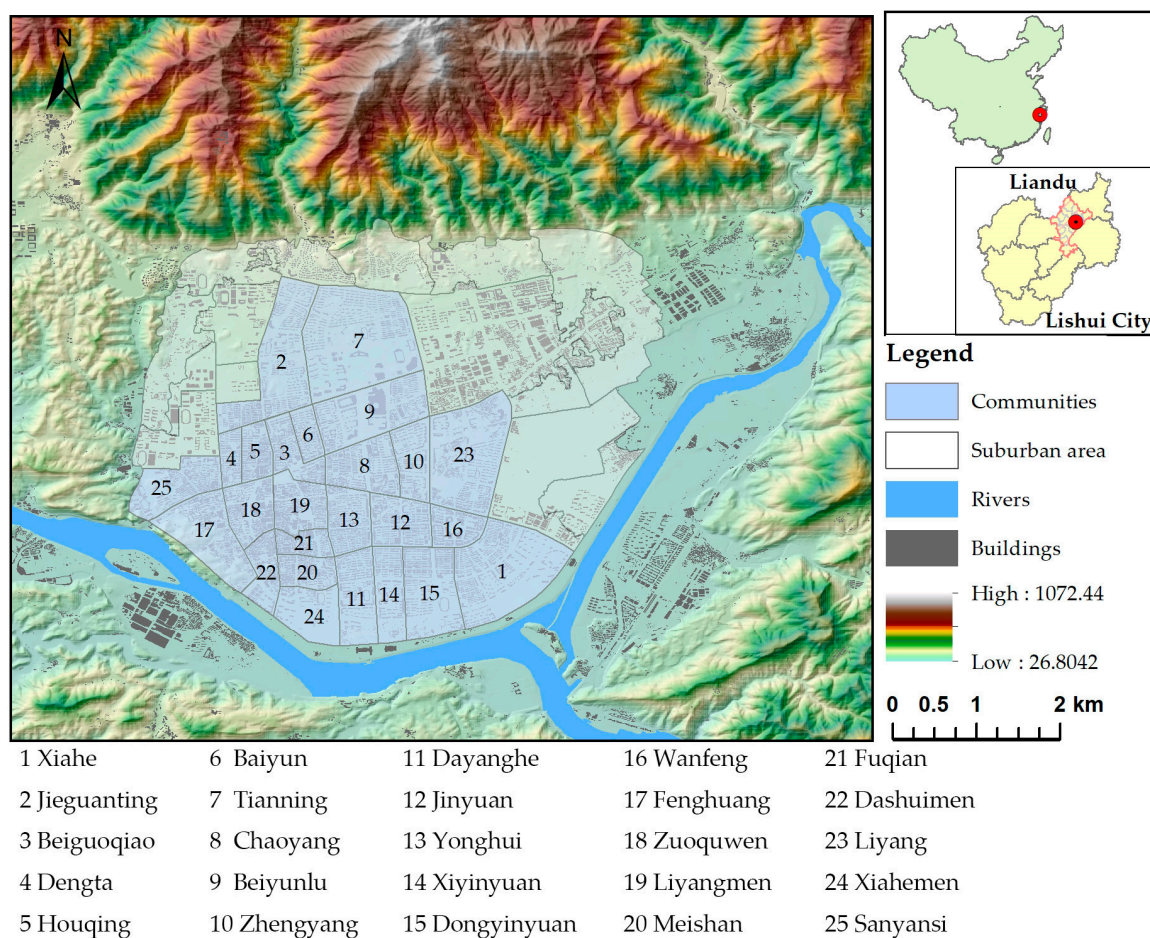


Figure 1. Location and communities of the study area.

From a hydrometeorological perspective, the area is vulnerable to different types of floods. First, the study area is a substantial fluvial-flood-affected area located in the confluence of the Haoxi River and the Daxi River in the middle and lower reaches of the Oujiang River basin. Upstream, the area is mountainous, and the river discharge is often very high during the rainy season. Liandu District features a subtropical monsoon climate and is high in annual precipitation (~1733 mm). June and July mark the rainy season, during which frequent and continuous rainfall occurs. During this season, local plums mature; thus, the period is called the plum rain season or East Asian rainy season, as it is the common climatic phenomenon in the eastern coastal regions of China. Although the city is not located in a coastal region, it is often affected by typhoons owing to its proximity to the East China Sea.

The most recent flood event in the study area occurred on 20 August 2014, when the entire Oujiang basin was hit by heavy and durative rainfall that induced a 50-year flood and caused considerable loss of economic property in the urban area.

2.2. Study Data

The vulnerability assessment was implemented using an indicator-based method, where indicators were derived from the results of flood modeling and existing physical, social, and economic data. Datasets were mainly used to create models with different flood scenarios and physical, social, and economic indicators for the vulnerability assessment.

A large amount of geographic and hydrometeorological data were used for the construction of the flood models. Terrain data and municipal drainage system data formed the essential framework of the flood models in this study. Terrain data, including digital elevation model data with 5 m resolution and river bathymetry data, were interpolated from river cross-section survey data provided by the Lishui Geographic Information Center (LSIC). Municipal drainage data, including central lines of rivers and channels, rainwater pipelines, and other drainage facilities, such as pumps and manholes, were also provided by the LSIC. Moreover, hydrometeorological data, which mainly include rainfall and river discharge, are important input parameters for flood modeling. Rainfall data were calculated using the local rainstorm intensity formula provided by the Lishui Meteorological Bureau:

$$q = \frac{1265.3(1 + 0.587LgP)}{(t + 5.919)^{0.611}}, \quad (1)$$

where q (mm/min) is the rainfall intensity, t (min) is the duration of rainfall, and P (years) is the return period of rainfall. The time series of river discharge and stage, including upstream and downstream, were obtained from the records of the local hydrological observatory during the latest 50-year flood on 20 August 2014.

Except for flood modeling, the indicators used to build indices were derived from abundant physical and socioeconomic data. The physical data were used to evaluate receptors that can be affected by floods, including buildings and various infrastructures, and most of these data were spatial data with locations and relevant attribute information. An example is the building data including the footprints and attributes, such as floor number, building area, and usage. Moreover, POI data provided by the LSIC were used as an important data source for increased access to urban infrastructure data. Thus, sufficient infrastructure information, such as the locations and attributes of retail stores, schools, nursing homes, plants, and basements, were extracted from POI data used to produce relevant indicators. Much of the social and economic information was collected from local statistical yearbooks and interviews with local community staff.

2.3. Methodological Outline

According to a report of the Intergovernmental Panel on Climate Change (IPCC), vulnerability can be regarded as a function of exposure, sensitivity, and adaptive capacity—expressed as Equation (2) [22,34,35]—and we use this as the framework of this study:

$$\text{Vulnerability} = f(E, S, AC), \quad (2)$$

where E represents exposure, S represents sensitivity, and AC represents adaptive capacity.

For flood disasters, vulnerability is the tendency towards an adverse effect of the flood. Exposure refers to the elements exposed to flood hazards in a specific region, such as people, buildings, infrastructure, and other personal or public assets. Many studies regard that all receptors can be affected by a disaster in the study area; that is, all receptors should be used for exposure assessment, no matter where they are located [10,36]. In our view, exposure should depend on a specific disaster. For example, the former approach is suitable for disasters with widespread effects, such as earthquakes.

However, for disasters where the scope of the effect can be determined, such as floods, the exposure of a population or infrastructure is determined by the extent of flooding and can vary under different flood hazards. Sensitivity is the intrinsic predisposition of an element to be affected by or susceptible to damage with the occurrence of a flood hazard. Adaptive capacity represents the ability of communities, institutions, or people to adjust to the flood, take advantage of opportunities, or respond to consequences. Based on this understanding of vulnerability to urban flooding, the research outline for this study was developed (Figure 2). Different types of urban flooding were simulated using a coupled flood model, which was built using LISFLOOD-FP [37] and the stormwater management model (SWMM) [38]. Flood simulation results were combined with variables to create a set of vulnerability indicators. Components of vulnerability, including exposure, sensibility, and adaptive capacity, were combined from the corresponding indicators using the AHP method. Finally, the vulnerability index was integrated from its components by using the WLC method. In this approach, GIS techniques and methods are frequently used in flood simulation and assessment as a spatial data processing method.

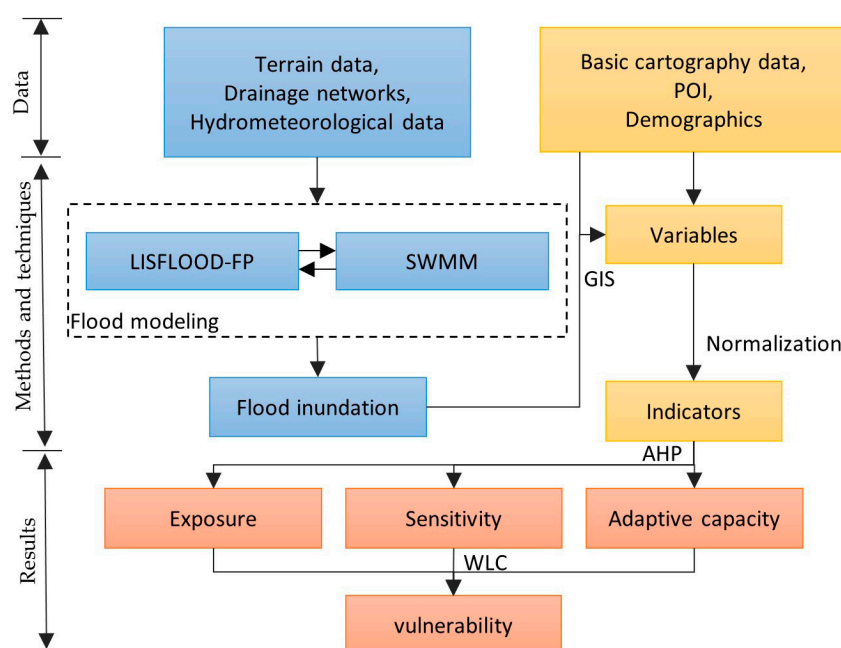


Figure 2. Outline of the flood vulnerability assessment approach.

2.4. Flood Modeling

2.4.1. Coupled Urban Flood Model

The SWMM is a dynamic urban flood simulation model widely used for the simulation of flooding and water quality in urban areas. The SWMM model includes a hydrological rain–runoff model and a 1D hydrodynamic model for simulation of municipal drainage networks, and is frequently used for urban planning, analysis, and design relevant to urban stormwater management. Although the SWMM can handle the interaction between surface runoff and sewer network runoff, the model cannot intuitively reveal the condition of flood inundation on the surface caused by overflow when the runoff exceeds the capacity of the rainwater drainage networks. A 2D hydrodynamic model, LISFLOOD-FP, was coupled with the SWMM model to solve this problem. LISFLOOD-FP is a highly efficient 2D hydrodynamic model used to simulate surface land inundation and fluvial floods; it can adapt to various complex terrains suited for the urban environment. Moreover, LISFLOOD-FP is a raster-based model; the regular grid is used as a computational unit to simulate 2D flood inundation and the sub-grid channel method is used to simulate the 1D river. Details of the coupling technique and implementation can be found in the literature [31–33]. To ensure model accuracy, our model coupling LISFLOOD-FP

and SWMM was validated using the observation records of the 2014 50-year flood. Meanwhile, field observations were carried out in communities 1 and 13, in which the urban area is ungauged. The verification process is described in detail in the literature [39,40]. The coupled urban flood model, which integrates characteristics of different models, not only adapts to the urban environment, but can also express urban floods intuitively and visually, which is important for urban risk and vulnerability analysis. In this study, the model was applied to urban flooding under different scenarios.

2.4.2. Urban Flood Scenarios

Considering the local physical environment and hydrometeorological characteristics, three types of floods were considered (pluvial, fluvial, and compound). Pluvial floods were induced by storm rainfall and included seven scenarios based on Equation (1), namely 1-, 5-, 10-, 20-, 30-, 50-, and 100-year rainfall. Fluvial floods were induced by river levee overtopping and were simulated based on the 50-year flood event of 20 August 2014. Compound flooding was induced by rainfall and river overtopping. The compound flood scenarios were simulated with different rainfall events and the river flood event of 20 August 2014. Meanwhile, a method based on GIS was used to directly combine the simulation results of urban pluvial flooding and fluvial flooding to allow for comparison with the flood modeling method. Therefore, compound flooding was obtained by the flood modeling and GIS methods.

2.5. Vulnerability Assessment

The indicator-based method was used for vulnerability assessment. The indicators were selected and integrated based on the vulnerability framework, as shown in Equation (2). The selected vulnerability indicators were divided into three, namely exposure, sensitivity, and adaptive capacity. Finally, the sub-indices were integrated into a comprehensive vulnerability index.

Using a method of combining the flood model and GIS techniques, the level of exposure was determined by the receptors (i.e., the factors that suffer adverse effects from urban flooding within the community, such as populations and buildings). In this method, the results of flood modeling were simulated for the given flood scenario, including water depth and extent of flooding, and then overlaid on other spatial data layers, such as populations and buildings, to determine the affected elements. Then, the exposure elements were identified and counted in each neighborhood based on GIS methods and selected as exposure variates.

Sensitivity is related to physical, social, and economic weaknesses and disadvantages. For urban flooding, sensitivity indicators should indicate vulnerable places and socioeconomic receptors for the flood disaster. Moreover, the sensitivity indicator was divided into two categories, namely physical and socioeconomic sensitivity. For physical sensitivity, indicators were used to reveal areas and places vulnerable to flooding. Several flood-related indicators were selected, including elevation, slope, distance to channels, and reservoirs, to identify sensitive areas. Then, places vulnerable to urban flooding in each community, such as elementary schools, nursing homes, basements, and chemical plants, were counted. For socioeconomic sensitivity, the sensitive population, including the disabled, aged, children, and those on a low-income (i.e., those who receive social assistance), was selected as an indicator; the data on these groups were obtained from the Lishui City Statistics Bureau.

Adaptive capacity is the ability to adapt to a disaster. In this study, the convenience of obtaining rescue and help was used to assess the adaptive capacity when facing the threat of floods. Therefore, rescue and medical services, including hospitals, shelters, and police and fire stations, were selected, and these data were converted into indicators based on a GIS method of Euclidean distance analysis.

The selected indicators were normalized to process them under a unified framework and make the evaluation results comparable. In this study, the United Nations Development Program's (UNDP) Human Development Index normalization method was used to process data and obtain indicators free of units and scales [41]. Through normalization, each indicator is assigned a value between 0 and 1. Based on the relationship between indicators and the corresponding object of evaluation, different normalization methods were selected. First, indicators were classified as having a positive or negative

relationship with the corresponding sub-index, including exposure, sensitivity, and adaptive capacity. In the assessment of exposure and adaptive capacity, all indicators were positive and enhanced the exposure and adaptive capacity by increasing the indicator value; the normalization was processed using Equation (3). However, the sensitivity of several indicators can decrease as the increasing indicator value increases; we used Equation (4) for normalization. Other positive indicators were also processed using Equation (4).

$$x'_i = \frac{x_i - x_{\min}}{x_{\max} - x_{\min}}, \quad (3)$$

$$x'_i = \frac{x_{\max} - x_i}{x_{\max} - x_{\min}}, \quad (4)$$

where x'_i is the x_i value of the indicator i after normalization, and x_{\max} and x_{\min} are the maximum and minimum values of the corresponding indicator, respectively.

$$V_{sub} = \sum_{i=1}^n w_i x'_i, \quad (5)$$

where V_{sub} is the sub-index of vulnerability, including exposure, sensitivity, and adaptive capacity, x'_i is the value of indicator i , and w_i is its weight.

After the development of indicator sets for each component of vulnerability, the AHP method, which is a multi-criteria decision-making (MCDM) technique initially introduced by Saaty [42], was used to assign weights to each indicator. AHP works well with GIS and was the main method for indicator integration in this study. Although AHP is a relatively subjective method, it can handle different insights from different perspectives, and allows decision-makers to change a complex problem into a hierarchical structure by identifying relationships between indicators. Therefore, AHP–GIS is frequently used in flood risk and vulnerability research [43]. Other methods to determine index weights are available, such as the entropy weight method, which is an objective method because the weight is determined by the corresponding indicator data. However, flood experience cannot be considered, and the relationships between indicators are ignored. Therefore, the AHP is considered a reasonable method for this study.

In this study, AHP was used as a weighted linear summation method in which the weight of an indicator was gained through pairwise comparison of the variable in a level of decision-making, and the sub-index was obtained from Equation (5). The final selected indicators and their corresponding weights are shown in Table 1. Finally, the WLC method was used to construct the sub-index and obtain the integrated vulnerability index, as shown in Equation (6):

$$V = Ew_E + Sw_S + ACw_{AC}, \quad (6)$$

where V , E , S , and AC are the vulnerability, exposure, sensitivity, and adaptive capacity, respectively; w_E , w_S , and w_{AC} are the corresponding weights, with values 0.5, 0.25, and 0.25 in this study, respectively [44].

Table 1. Variables and weights for urban flood vulnerability assessment.

Vulnerability Dimension	Dimension Weighting	Variable	Description	Variable Weighting
Exposure	0.5	Flooding area	Inundated area	0.193
		Population	Flood-affected population	0.544
		Commercial stores	Number of commercial stores in the flooding area	0.193
		Building area	Area of structure, area of building footprint multiplied by number of floors	0.07

Table 1. Cont.

Vulnerability Dimension	Dimension Weighting	Variable	Description	Variable Weighting
Sensitivity	0.25	Disabled population	Population of disabled people in the community	0.203
		Elderly population	Population of people above the age of 65 in the community	0.156
		Children	Population of people under the age of 12	0.150
		Low-income population	Population which receive basic living allowance from the local government	0.083
		Elementary School	Number of elementary schools in the community	0.136
		Nursing home	Number of nursing homes in the community	0.126
		Distance to the chemical plant	Number of plants that can cause environmental pollution after flooding	0.043
		Basement	Number of basements in community buildings	0.043
		Channel	Average distance to river channel for the community	0.020
		Elevation Reservoir	Average elevation in the community Average distance to nearest reservoir	0.020 0.020
Adaptive capacity	0.25	Flood risk awareness	Number of floods in the community	0.153
		Hospital	Average distance to hospitals	0.315
		Emergency shelter	Average distance to emergency shelters	0.409
		Rescue station	Average distance to police and fire stations	0.123

3. Results

3.1. Flood Modeling

Flooding maps, which were obtained from the results of urban flood modeling, display areas affected by different types of urban floods. This study extracted the maximum modeled floodwater depth at each location as the hazard factor; this was, then, used to identify the population and infrastructure in the hazardous areas to identify the worst-case flood scenario.

Pluvial and fluvial flooding have different causes. In general, urban pluvial flooding is caused by rainfall exceeding the drainage capacity of the city and always occurs in low-lying areas (e.g., community 13 of Lishui City), whereas fluvial flooding occurs due to river levee overtopping. In Lishui City, pluvial flooding is widely distributed in a discontinuous fashion across many communities (Figure 3a–g), including the urban center and suburban areas, and it continues to extend with increasing rainfall. In contrast, the 2014 50-year fluvial flood was continuously distributed in the low-lying area along the river (Figure 3h). As pluvial and fluvial flooding have different distribution characteristics, combining rainfall with river overtopping (i.e., compound flooding; Figures 4 and 5) has a significant effect on the spatial extent of the inundation area.

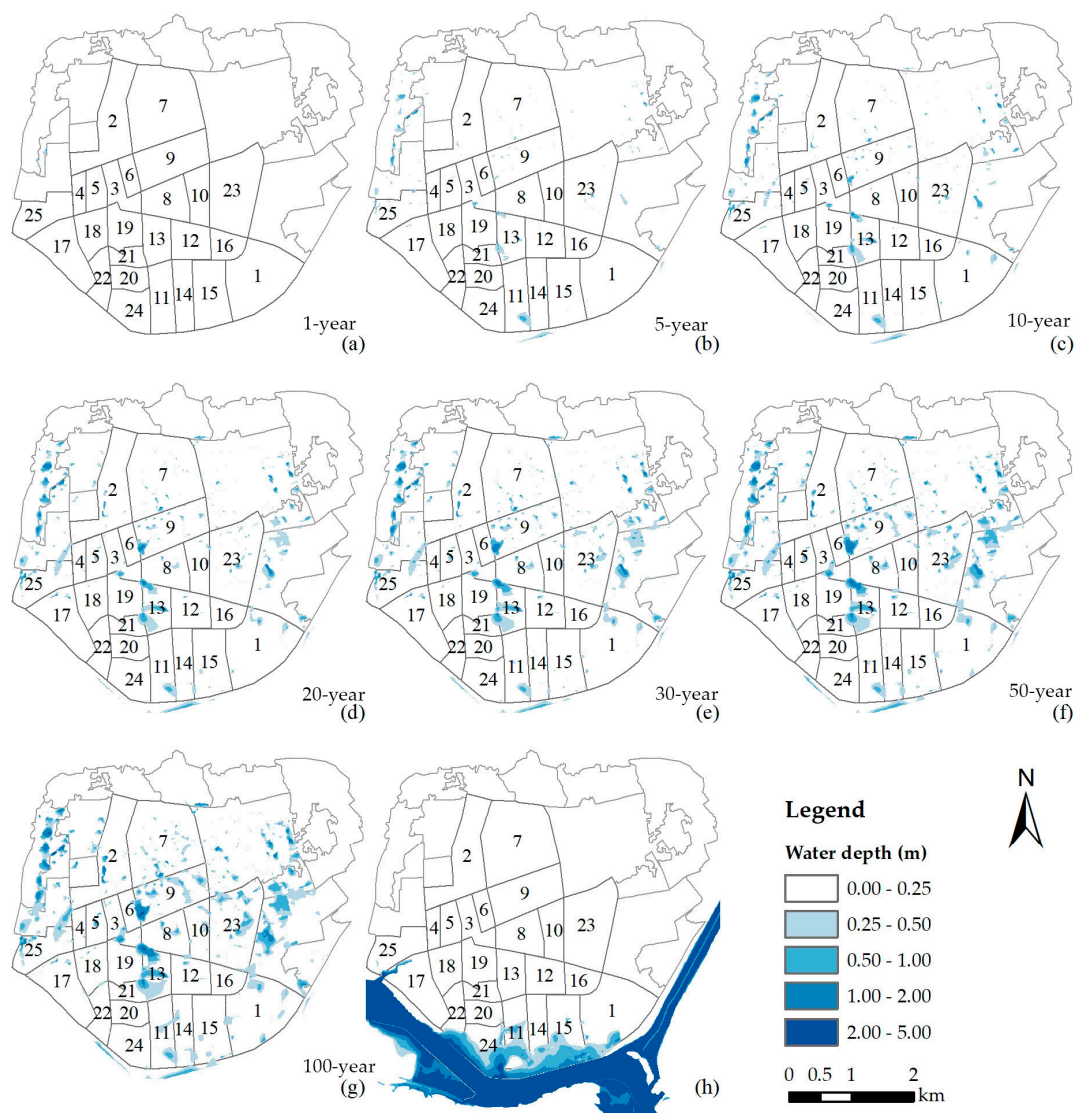


Figure 3. Modeled flood maps of pluvial flooding in Lishui City, China. (a–g) Pluvial floods following (a) 1-, (b) 5-, (c) 10-, (d) 20-, (e) 30-, (f) 50-, and (g) 100-year rainfall; (h) map of the 2014 50-year fluvial flood.

In Figure 6, the modeling output shows that pluvial flooding following a one-year rainfall had minimal effects on communities; only one community was slightly affected. However, as the rainfall intensity reached that of five year rainfall, the number of affected communities increased to 22, although the water depth remained shallow (Figure 6a). As the rainfall increased, the water depth and the range of pluvial flooding gradually increased. For 50-year rainfall, almost all communities were threatened by urban pluvial flooding. However, the increase in flooding area was relatively slow compared to that in the flood-affected communities. During the 2014 50-year fluvial flood, nine communities were affected, and are represented by a horizontal line in Figure 6 because only one pluvial flood scenario was designed in this study.

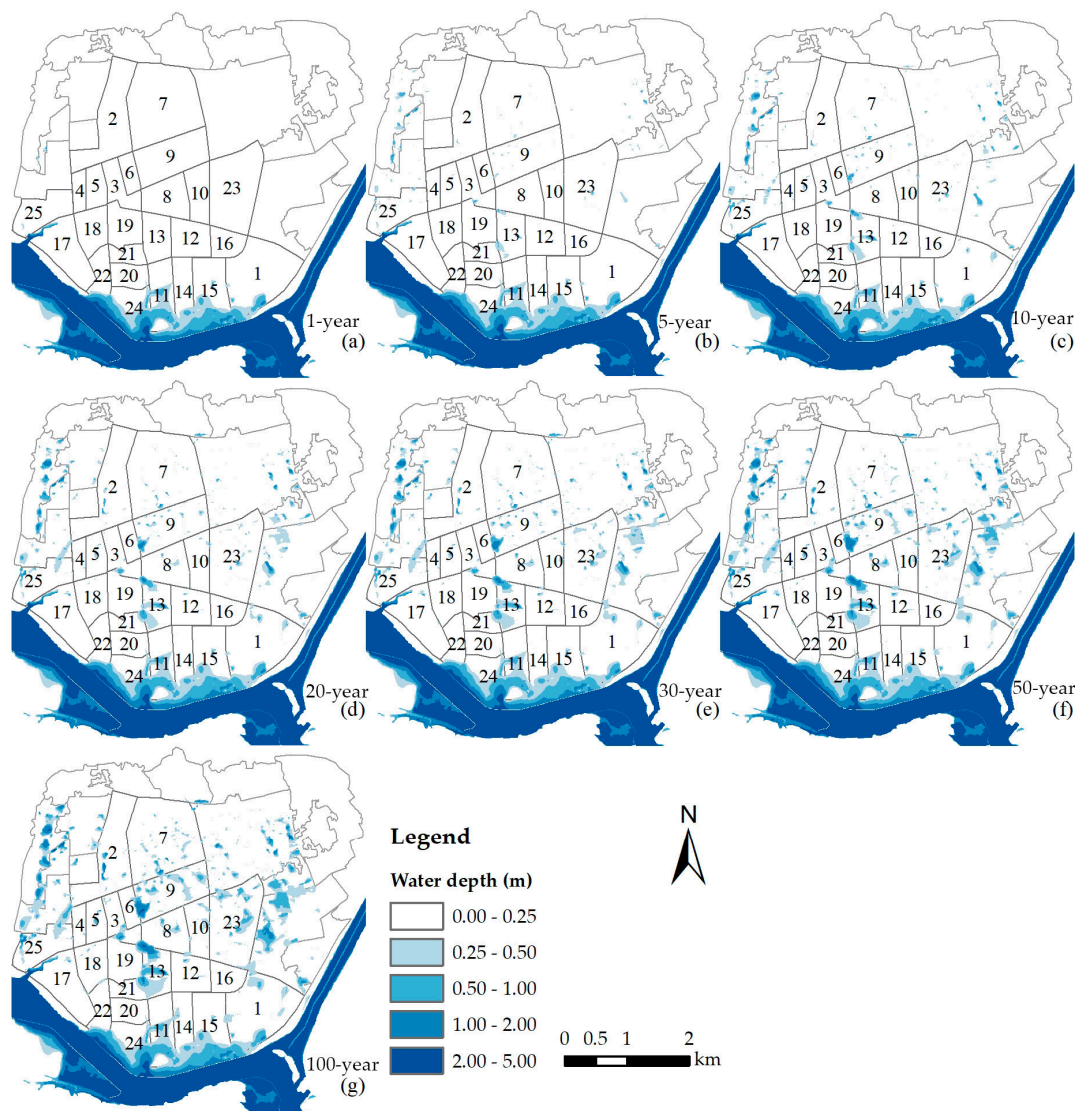


Figure 4. Flood maps of compound flooding in Lishui City, China from the geographical information system (GIS) analysis. (a–g) Compound floods following (a) 1-, (b) 5-, (c) 10-, (d) 20-, (e) 30-, (f) 50-, and (g) 100-year rainfall combined with the 2014 50-year fluvial flood.

For compound flooding, we compared two methods: GIS and flood modeling. Flooding caused by a combination of rainfall and river overtopping represented the most severe urban flood scenario. Inundation occurred in almost every community following the 20-year rainfall combined with fluvial flooding. Overall, the results of pluvial and compound flooding displayed the same trends under the influence of serial rainfall.

Given the combined effects of rainfall and fluvial flooding, compound floods are more serious than the pluvial flood. Nine communities were affected by more serious flooding than pluvial flooding, with fluvial flooding being the dominant contributor. However, compound and pluvial flooding results were similar when rainfall was 20-year rainfall or less (Figure 6b), with the curve from the modeling method located above that of the GIS method. Thus, the modeling of compound flooding shows a greater flood impact than the GIS method.

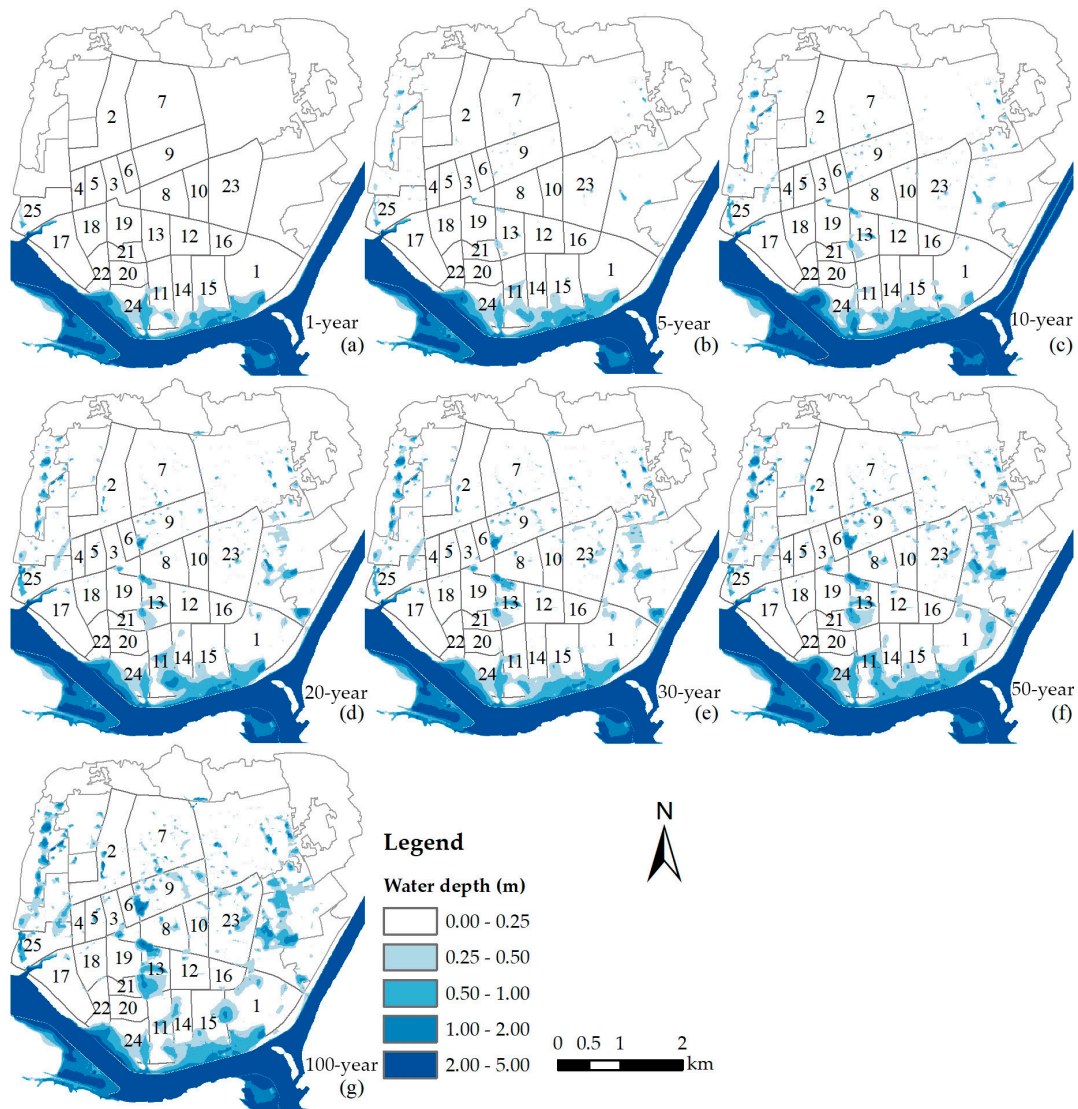


Figure 5. Flood maps of compound flooding in Lishui City, China from the geographical information system (GIS) analysis. (a–g) Compound floods following (a) 1-, (b) 5-, (c) 10-, (d) 20-, (e) 30-, (f) 50-, and (g) 100-year rainfall combined with the 2014 50-year fluvial flood.

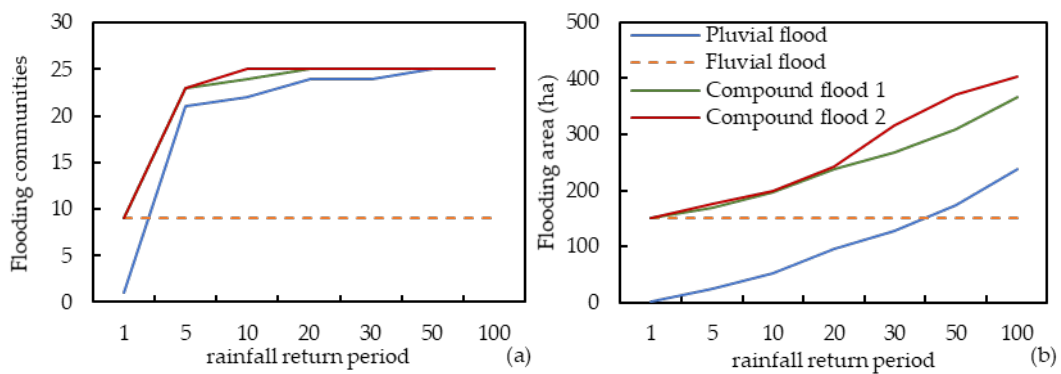


Figure 6. Numbers of (a) flood-affected communities and (b) flooding areas for different types of urban flooding under different scenarios. Compound floods 1 and 2 are the results of compound flooding using the GIS and modeling methods, respectively.

3.2. Exposure

Based on the distribution results, exposure was divided into five levels: very low, low, medium, high, and very high. Community exposures to different types of floods are shown in Tables 2–4.

Table 2. Community exposure to pluvial and fluvial flooding.

Exposure Level	Rainfall							Fluvial Flood
	1-Year	5-Year	10-Year	20-Year	30-Year	50-Year	100-Year	
Very Low [0.0–0.2]	All	All	Others	Others	Others	Others	Others	Others
Low (0.2–0.4)	-	-	13	13	9	1, 9, 23	1, 7	1, 14
Medium (0.4–0.6)	-	-	-	-	13	13	9, 13, 23	11, 15, 24
High (0.6–0.8)	-	-	-	-	-	-	-	-
Very high (0.8–1.0)	-	-	-	-	-	-	-	-

Table 3. Community exposure to compound flooding according to the GIS method.

Exposure Level	Combined Fluvial and Pluvial Flooding According to Rainfall Level						
	1-Year	5-Year	10-Year	20-Year	30-Year	50-Year	100-Year
Very Low [0.0–0.2]	Others	Others	Others	Others	Others	Others	Others
Low (0.2–0.4)	1, 14	1, 14	1, 13, 14	1, 13, 14	9, 14	9, 14, 23	7, 14
Medium (0.4–0.6)	11, 15, 24	11, 15, 24	11, 15, 24	11, 15, 24	1, 11, 13, 15, 24	1, 11, 13, 15, 24	1, 9, 11, 13, 15, 23, 24
High (0.6–0.8)	-	-	-	-	-	-	-
Very high (0.8–1.0)	-	-	-	-	-	-	-

Table 4. Community exposure to compound flooding according to the flood modeling method.

Exposure Level	Combined Fluvial and Pluvial Flooding According to Rainfall Level						
	1-Year	5-Year	10-Year	20-Year	30-Year	50-Year	100-Year
Very Low [0.0–0.2]	Others	Others	Others	Others	Others	Others	Others
Low (0.2–0.4)	1, 14	1, 14	1, 13, 14	13, 14	9, 14	9, 14, 23	14
Medium (0.4–0.6)	11, 15, 24	11, 15, 24	11, 15, 24	1, 11, 15, 24	1, 11, 13, 15, 24	11, 13, 24	9, 11, 23, 24
High (0.6–0.8)	-	-	-	-	-	15	13, 15
Very high (0.8–1.0)	-	-	-	-	-	1	1

Comparing communities with different exposure levels, exposure shows obvious differences among different flood types. For pluvial flooding (Table 2), when the rainfall intensity was that of 20-year rainfall or less, all communities were at very low and low exposure levels. When rainfall intensity increased to that of 30-year rainfall, community 13 shifted to medium exposure. As rainfall intensity increased to that of 100-year rainfall, three communities were at a medium exposure level. For fluvial flooding, there were three communities at a medium exposure level. For compound flooding, under the combined effects of the two flood factors, the number of communities at medium or higher exposure levels increased significantly. When rainfall intensity was that of 20-year rainfall or less in the compound floods, the number of communities with medium exposure was similar to that in the fluvial

flood scenario. More than 20% of the communities were at medium or higher exposure levels for the worst compound flood scenario. There were also differences among the compound floods obtained using the different methods. In particular, for rainfall intensity of 50- or 100-year rainfall, communities with high and very high exposure appeared in the results of flood modeling.

Considering the spatial locations of communities, the spatial distributions of exposure also differed for different types of floods. Communities with medium or higher exposure levels (communities 9, 13, 23) appeared in urban centers when the rainfall intensity was that of 30-year rainfall and in the suburban areas when rainfall intensity reached that of 100-year rainfall. Overall, only a few communities had medium or high exposure as a result of pluvial flooding, and these were mainly distributed in local low-lying areas. In terms of fluvial flooding, the three communities with medium exposure were distributed along the river. For compound flooding, communities with medium or higher exposure appeared in the city center and suburban areas simultaneously.

3.3. Sensitivity and Adaptive Capacity

The results of sensitivity and adaptive capacity were divided into four levels using the natural break method (Jenks) [45], as shown in Figure 7. For sensitivity, six communities were at a high level, seven communities were at medium levels, and the remaining were at low and very low levels. All high-sensitivity communities were located in the central urban area, except for community 15, whereas the communities with low and very low sensitivity were located on the edges of the urban area. For adaptive capacity, five communities with high adaptive capacity formed two high-value areas within the city; these communities had easy access to health services and shelters. Communities with low and very low adaptive capacity were predominantly located in the suburban and riverine areas, far from shelters.

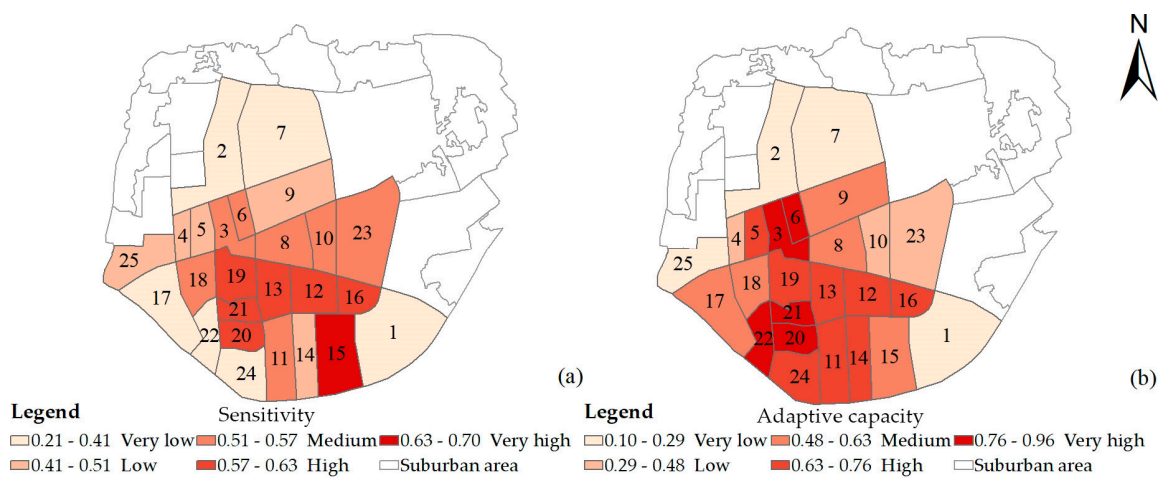


Figure 7. Maps of community (a) sensitivity and (b) adaptive capacity.

3.4. Vulnerability Assessment

Based on the assessment of exposure, sensitivity, and adaptive capacity, the vulnerability was integrated using WLC. The vulnerability was also divided into five levels, namely very low, low, medium, high, and very high. The results are shown in Tables 5–7.

Table 5. Pluvial and fluvial flood vulnerability.

Vulnerability Level	Rainfall							Fluvial Flood
	1-Year	5-Year	10-Year	20-Year	30-Year	50-Year	100-Year	
Very Low [−0.25−0.05]	3, 6, 14, 20, 21, 22, 24	3, 6, 14, 20, 22, 24	3, 6, 14, 20, 22, 24	3, 6, 20, 22, 24	6, 20, 22, 24	6, 20, 22, 24	6, 20, 22, 24	3, 6, 20, 21
Low (−0.05−0.15]	Others	Others	Others	Others	Others	Others	Others	Others
Medium (0.15−0.35]	-	-	-	-	13, 25	1, 9, 13, 23, 25	1, 9, 13, 23, 25	1, 11, 15, 24
High (0.35−0.55]	-	-	-	-	-	-	-	-
Very high (0.55−0.75]	-	-	-	-	-	-	-	-

Table 6. Vulnerability of compound flooding according to the GIS method.

Vulnerability Levels	Combined Fluvial and Pluvial Flooding According to Rainfall Level						
	1-Year	5-Year	10-Year	20-Year	30-Year	50-Year	100-Year
Very Low [−0.25−0.05]	3, 6, 20, 21	3, 6, 20	3, 6, 20	6, 20	6, 20	6, 20	6, 20
Low (−0.05−0.15]	Others	Others	Others	Others	Others	Others	Others
Medium (0.15−0.35]	1, 11, 15, 24	1, 11, 15, 24	1, 11, 15, 24	1, 11, 15, 24	1, 11, 13, 15, 24, 25	1, 9, 11, 13, 15, 23, 24, 25	1, 9, 11, 13, 15, 23, 24, 25
High (0.35−0.55]	-	-	-	-	-	-	-
Very high (0.55−0.75]	-	-	-	-	-	-	-

Table 7. Vulnerability of compound flooding according to the flood modeling method.

Vulnerability Levels	Combined Fluvial and Pluvial Flooding According to Rainfall Level						
	1-Year	5-Year	10-Year	20-Year	30-Year	50-Year	100-Year
Very Low [−0.25−0.05]	3, 6, 20, 21, 22	3, 6, 20, 22	3, 6, 20	3, 6, 20	6, 20	6, 20	6, 20
Low (−0.05−0.15]	Others	Others	Others	Others	Others	Others	Others
Medium (0.15−0.35]	1, 11, 15, 24	1, 11, 15, 24	1, 11, 15, 24, 25	1, 11, 13, 15, 24, 25	1, 11, 13, 15, 24, 25	9, 11, 13, 23, 24, 25	9, 11, 13, 23, 24, 25
High (0.35−0.55]	-	-	-	-	-	1, 15	15
Very high (0.55−0.75]	-	-	-	-	-	-	1

Community vulnerability varied for different urban flood scenarios. For pluvial flooding (Table 5), when rainfall intensity was that of 20-year rainfall or less, all communities had low or very low vulnerability levels. We found that 20% of communities had a medium vulnerability in the worst compound flood scenario. No communities had high or very high vulnerability for the pluvial flood. For fluvial flooding (Table 5), four communities had a medium vulnerability, and there were no high-vulnerability communities. For compounding flood according to the GIS method (Table 6), when rainfall intensity was that of 20-year rainfall or less, the number of communities with medium vulnerability was similar to that for fluvial or pluvial flooding when the rainfall intensity reached that of 50- or 100-year rainfall. Compound flood vulnerability with flood modeling showed an increase in the number of communities with high or very high vulnerability levels.

According to the spatial distribution of vulnerability, for pluvial flooding, initially, communities with medium vulnerability were almost distributed in suburban areas, except for community 13 (city center). For fluvial flooding, all medium-vulnerability communities were distributed along the river. For compound flooding according to the GIS method, the distribution was the same as that for the superposition of pluvial and fluvial flooding. Most communities with medium or higher vulnerability

were located in suburban areas or along the river. The vulnerabilities to compound flooding using the modeling method had a similar distribution to those using the GIS method.

4. Discussion

Assessing community vulnerability to urban flooding, which is important for flood hazard mitigation planning, requires the identification of vulnerable communities and factors that can increase the vulnerability. The results of this study suggest that the vulnerabilities of different communities within the same city vary considerably owing to the physical and socioeconomic gaps; the different vulnerability levels can be distinguished by analyzing the results of flood modeling and vulnerability assessment. Flood and vulnerability maps display the exposure and vulnerability of communities to different types of floods, can help city management departments and decision-makers in developing flood mitigation and adaptation strategies on a community scale, and can reduce the adverse effects of urban flooding in an efficient and target-specific manner.

The results of this study have implications for the methods and theory of vulnerability studies. First, a coupled flood model combined with GIS techniques was applied to map different types of floods and the relationships with physical and social indicators; from this, it was possible to map exposure, sensitivity, and adaptive capacity, and then to create a composite vulnerability index using the AHP and WLC methods. In particular, the assessment of exposure is linked to the flood hazard, and the results were consistent with reality; that is, the flood was more severe when a large population and more infrastructure were affected. Therefore, the exposure and vulnerability under different flood scenarios, which can help in flood management according to actual local conditions, are critical. This study addressed a gap in urban flood vulnerability research concerning different types of floods, including compound flooding induced by rainfall and river flooding. Currently, most flood vulnerability studies are focused on floods caused by single factors, such as river overtopping or storm surges. There are numerous vulnerability studies of river flooding with even the term “flood” commonly being defined as a river-related phenomenon. This study substantially differs from others because it simultaneously considered pluvial and fluvial floods (induced by rainfall and river overtopping, respectively) and analyzed the effects of these different flood types on vulnerabilities of urban communities by reexamining the theoretical basis of the “place-based” vulnerability and GIS methods [21,22,46,47].

Community vulnerability to different types of floods has different characteristics. The results of exposure show that fluvial flooding has a more substantial effect on riverine communities compared to pluvial flooding induced by 30-year or less rainfall. Therefore, fluvial flooding is frequently studied in vulnerability research. However, pluvial flooding can have an effect comparable to that of fluvial flooding when the rainfall intensity reaches that of 50- or 100-year rainfall, which is similar to the findings of existing studies [12]. Pluvial flooding and urban pluvial flooding can have intersections and interactions, such as compound flooding induced by rainfall and river flooding. Compound flooding has the most severe effect on the three types of communities because it has a wider distribution, reflecting the fact that fluvial and pluvial floods can have substantially different impact areas. Moreover, compound flooding results in more medium- and high-vulnerability communities. The vulnerability of communities to flooding can be underestimated when compound flooding is not considered. Multiple or compound hazards are increasing owing to climate change [18,20], and the assessment of compound flood vulnerability is necessary to aid communities to cope with possible future flood disasters.

The results of this study suggest that urbanization contributes to increased flood vulnerability. In the study area, increased infrastructure, such as hospitals and shelters in the urban center area, can enhance the adaptive capacity of a community, as nearby communities can easily access these services. Communities in suburban areas are less likely to be adaptive owing to the greater distance from infrastructure facilities. Thus, infrastructure development should meet the needs of urban communities; otherwise, communities within newly developed areas may become more susceptible to disasters. Central urban areas can be low-value aggregation areas of urban social vulnerability, whereas

surrounding areas have a high-value aggregation of social vulnerability [48]. Moreover, this study provides suggestions for more effective urban flood management and urban planning. Our spatial vulnerability assessment approach can identify areas and communities vulnerable to urban flooding. Different response measures should be implemented according to the level of vulnerability and flood type. For example, dams along the river in communities 11, 14, 15, and 24 need to be strengthened, low-impact development measures should be carried out in community 13, and more medical facilities and shelters are needed in suburban areas.

The method used in this study is limited because of its high dependency on the flood modeling and the limited availability of socioeconomic data. Although the coupled model is a well-established technique that is widely used in flood risk and vulnerability studies, the calibration and validation are still characterized by uncertainty. Therefore, more validation should be done to verify the model further. In flood modeling, the influence of river water level on urban drainage is important; however, in this study, only one fluvial flood scenario was used (i.e., the worst fluvial flood scenario). This was chosen because flood modeling and flood hazards were not the focus of this research; however, the complexity and influencing factor combinations of more compound flood scenarios should be studied in the future. Data are a crucial constraint in vulnerability studies. For this reason, we selected POI data, whose collection requires manual data evaluation. However, vulnerability research requires current and real-life data, especially for communities with small amounts of demographic and socioeconomic statistics, and POI data may have a timeliness issue; for example, errors caused by POI data are not updated on time.

5. Conclusions

This study outlined an integrated method for the assessment of community vulnerability to urban flooding based on flood modeling and GIS. Modeling of various urban flood scenarios, including fluvial, pluvial, and compound flooding, was carried out to reveal the level of vulnerability to different types of urban floods. The method was applied to Lishui, Zhejiang, China; however, it could be used in other cities owing to its strong replicability. The flood modeling results show that different types of flood can occupy different areas and have adverse effects: Pluvial urban floods can occur in many parts of a city, fluvial flooding mainly affects areas along rivers, and compound flooding combines rainfall with river overtopping; it has a wider range of effects and can be more serious than the simple accumulation of fluvial and pluvial flooding. Exposure assessment based on flood modeling quantified the affected population and infrastructure. Sensitivity and adaptive capacity reflect the effect of a community's socioeconomic status on its flood vulnerability. The spatial distributions of the two were found to be similar; that is, urban centers tend to have higher sensitivity and adaptive capacity, and the opposite is true for suburban areas. Flood vulnerability assessment is a composite of multiple effects, including disaster, socioeconomic factors, and vulnerability, indicating that different flood vulnerabilities have substantially varied effects. Compound flood vulnerability is higher than single-factor flood vulnerability, especially in regions where multiple factors are combined.

The results of this study can guide urban managers and policymakers on community flood management. These results revisit the gaps in current flood measures and provide guidance to reduce vulnerability. Further validation of the assessment results is required in future studies, including those on flood simulation and vulnerability.

Author Contributions: Conceptualization, Q.Y.; Methodology and Data Analysis, Q.Y.; Visualization, Q.Y.; Writing—Original Draft Preparation, Q.Y.; Writing—Review and Editing, R.Y., Q.Y., and S.Z.; Supervision, S.Z. and Q.D. All authors have read and agreed to the published version of the manuscript.

Funding: This research was funded by the National Natural Science Foundation of China, grant numbers 41771424 and 41871299.

Acknowledgments: Special thanks are due to the Lishui Geographic Information Center for providing topographic data and sewer network data of the case study area.

Conflicts of Interest: The authors declare no conflict of interest.

References

1. Ziegler, A.D. Reduce urban flood vulnerability. *Nature* **2012**, *481*, 145. [[CrossRef](#)] [[PubMed](#)]
2. Paprotny, D.; Sebastian, A.; Morales-Napoles, O.; Jonkman, S.N. Trends in flood losses in Europe over the past 150 years. *Nat. Commun.* **2018**, *9*, 1985. [[CrossRef](#)] [[PubMed](#)]
3. Khajehei, S.; Ahmadalipour, A.; Shao, W.; Moradkhani, H. A Place-based Assessment of Flash Flood Hazard and Vulnerability in the Contiguous United States. *Sci. Rep.* **2020**, *10*, 448. [[CrossRef](#)] [[PubMed](#)]
4. Ward, P.J.; Jongman, B.; Aerts, J.C.J.H.; Bates, P.D.; Botzen, W.J.W.; Diaz Loaiza, A.; Hallegatte, S.; Kind, J.M.; Kwadijk, J.; Scussolini, P.; et al. A global framework for future costs and benefits of river-flood protection in urban areas. *Nat. Clim. Chang.* **2017**, *7*, 642–646. [[CrossRef](#)]
5. Tyler, J.; Sadiq, A.-A.; Noonan, D.S. A review of the community flood risk management literature in the USA: Lessons for improving community resilience to floods. *Nat. Hazards* **2019**, *96*, 1223–1248. [[CrossRef](#)]
6. Sadiq, A.-A.; Tyler, J.; Noonan, D.S. A review of community flood risk management studies in the United States. *Int. J. Disaster Risk Reduct.* **2019**, *41*. [[CrossRef](#)]
7. Alves, A.; Gersonius, B.; Kapelan, Z.; Vojinovic, Z.; Sanchez, A. Assessing the Co-Benefits of green-blue-grey infrastructure for sustainable urban flood risk management. *J. Environ. Manag.* **2019**, *239*, 244–254. [[CrossRef](#)]
8. Chan, F.K.S.; Griffiths, J.A.; Higgitt, D.; Xu, S.; Zhu, F.; Tang, Y.-T.; Xu, Y.; Thorne, C.R. “Sponge City” in China—A breakthrough of planning and flood risk management in the urban context. *Land Use Policy* **2018**, *76*, 772–778. [[CrossRef](#)]
9. Thorne, C.R.; Lawson, E.C.; Ozawa, C.; Hamlin, S.L.; Smith, L.A. Overcoming uncertainty and barriers to adoption of Blue-Green Infrastructure for urban flood risk management. *J. Flood Risk Manag.* **2018**, *11*, S960–S972. [[CrossRef](#)]
10. Chang, S.E.; Yip, J.Z.K.; Conger, T.; Oulahan, G.; Marteleira, M. Community vulnerability to coastal hazards: Developing a typology for disaster risk reduction. *Appl. Geogr.* **2018**, *91*, 81–88. [[CrossRef](#)]
11. Wu, W.; McInnes, K.; O’Grady, J.; Hoeke, R.; Leonard, M.; Westra, S. Mapping Dependence Between Extreme Rainfall and Storm Surge. *J. Geophys. Res. Ocean.* **2018**, *123*, 2461–2474. [[CrossRef](#)]
12. Tanaka, T.; Kiyohara, K.; Tachikawa, Y. Comparison of fluvial and pluvial flood risk curves in urban cities derived from a large ensemble climate simulation dataset: A case study in Nagoya, Japan. *J. Hydrol.* **2020**, *584*. [[CrossRef](#)]
13. Andrade, M.M.N.; Szlafsztein, C.F. Vulnerability assessment including tangible and intangible components in the index composition: An Amazon case study of flooding and flash flooding. *Sci. Total Environ.* **2018**, *630*, 903–912. [[CrossRef](#)] [[PubMed](#)]
14. Tapia, C.; Abajo, B.; Feliu, E.; Mendizabal, M.; Martinez, J.A.; Fernández, J.G.; Laburu, T.; Lejarazu, A. Profiling urban vulnerabilities to climate change: An indicator-based vulnerability assessment for European cities. *Ecol. Indic.* **2017**, *78*, 142–155. [[CrossRef](#)]
15. Muthusamy, M.; Rivas Casado, M.; Salmoral, G.; Irvine, T.; Leinster, P. A Remote Sensing Based Integrated Approach to Quantify the Impact of Fluvial and Pluvial Flooding in an Urban Catchment. *Remote Sens.* **2019**, *11*, 577. [[CrossRef](#)]
16. Chen, A.S.; Djordjevic, S.; Leandro, J.; Savic, D.A. An analysis of the combined consequences of pluvial and fluvial flooding. *Water Sci. Technol.* **2010**, *62*, 1491–1498. [[CrossRef](#)] [[PubMed](#)]
17. Patra, J.P.; Kumar, R.; Mani, P. Combined Fluvial and Pluvial Flood Inundation Modelling for a Project Site. *Procedia Technol.* **2016**, *24*, 93–100. [[CrossRef](#)]
18. Hao, Z.; Singh, V.; Hao, F. Compound Extremes in Hydroclimatology: A Review. *Water* **2018**, *10*, 718. [[CrossRef](#)]
19. Wahl, T.; Jain, S.; Bender, J.; Meyers, S.D.; Luther, M.E. Increasing risk of compound flooding from storm surge and rainfall for major US cities. *Nat. Clim. Chang.* **2015**, *5*, 1093–1097. [[CrossRef](#)]
20. Paprotny, D.; Vousdoukas, M.I.; Morales-Nápoles, O.; Jonkman, S.N.; Feyen, L. Compound flood potential in Europe. *Hydrol. Earth Syst. Sci. Discuss.* **2018**, 1–34. [[CrossRef](#)]
21. Cutter, S.L.; Finch, C. Temporal and spatial changes in social vulnerability to natural hazards. *Proc. Natl. Acad. Sci. USA* **2008**, *105*, 2301–2306. [[CrossRef](#)]
22. Turner, B.L.; Kasperson, R.E.; Matson, P.A.; McCarthy, J.J.; Corell, R.W.; Christensen, L.; Eckley, N.; Kasperson, J.X.; Luers, A.; Martello, M.L.; et al. A framework for vulnerability analysis in sustainability science. *Proc. Natl. Acad. Sci. USA* **2003**, *100*, 8074–8079. [[CrossRef](#)] [[PubMed](#)]

23. Weis, S.W.M.; Agostini, V.N.; Roth, L.M.; Gilmer, B.; Schill, S.R.; Knowles, J.E.; Blyther, R. Assessing vulnerability: An integrated approach for mapping adaptive capacity, sensitivity, and exposure. *Clim. Chang.* **2016**, *136*, 615–629. [[CrossRef](#)]
24. Aroca-Jimenez, E.; Bodoque, J.M.; Garcia, J.A.; Diez-Herrero, A. Construction of an integrated social vulnerability index in urban areas prone to flash flooding. *Nat. Hazards Earth Syst. Sci.* **2017**, *17*, 1541–1557. [[CrossRef](#)]
25. Lins-de-Barros, F.M. Integrated coastal vulnerability assessment: A methodology for coastal cities management integrating socioeconomic, physical and environmental dimensions—Case study of Regido dos Lagos, Rio de Janeiro, Brazil. *Ocean Coast. Manag.* **2017**, *149*, 1–11. [[CrossRef](#)]
26. Gigović, L.; Pamučar, D.; Bajić, Z.; Drobnjak, S. Application of GIS-Interval Rough AHP Methodology for Flood Hazard Mapping in Urban Areas. *Water* **2017**, *9*, 360. [[CrossRef](#)]
27. Ghajari, Y.; Alesheikh, A.; Modiri, M.; Hosnavi, R.; Abbasi, M. Spatial Modelling of Urban Physical Vulnerability to Explosion Hazards Using GIS and Fuzzy MCDA. *Sustainability* **2017**, *9*, 1274. [[CrossRef](#)]
28. Hu, S.; Cheng, X.; Zhou, D.; Zhang, H. GIS-based flood risk assessment in suburban areas: A case study of the Fangshan District, Beijing. *Nat. Hazards* **2017**, *87*, 1525–1543. [[CrossRef](#)]
29. Martins, R.; Leandro, J.; Djordjević, S. Influence of sewer network models on urban flood damage assessment based on coupled 1D/2D models. *J. Flood Risk Manag.* **2018**, *11*, S717–S728. [[CrossRef](#)]
30. Mignot, E.; Li, X.; Dewals, B. Experimental modelling of urban flooding: A review. *J. Hydrol.* **2019**, *568*, 334–342. [[CrossRef](#)]
31. Wu, X.; Wang, Z.; Guo, S.; Liao, W.; Zeng, Z.; Chen, X. Scenario-based projections of future urban inundation within a coupled hydrodynamic model framework: A case study in Dongguan City, China. *J. Hydrol.* **2017**, *547*, 428–442. [[CrossRef](#)]
32. Chen, A.S.; Leandro, J.; Djordjević, S. Modelling sewer discharge via displacement of manhole covers during flood events using 1D/2D SIPSON/P-DWave dual drainage simulations. *Urban Water J.* **2015**, *13*, 830–840. [[CrossRef](#)]
33. Leandro, J.; Martins, R. A methodology for linking 2D overland flow models with the sewer network model SWMM 5.1 based on dynamic link libraries. *Water Sci. Technol.* **2016**, *73*, 3017–3026. [[CrossRef](#)]
34. Parry, M.; Parry, M.L.; Canziani, O.; Palutikof, J.; Van der Linden, P.; Hanson, C. *Climate Change 2007-Impacts, Adaptation and Vulnerability: Working Group II Contribution to the Fourth Assessment Report of the IPCC*; Cambridge University Press: Cambridge, UK, 2007; Volume 4.
35. Maleki, R.; Nooripoor, M.; Azadi, H.; Lebailly, P. Vulnerability Assessment of Rural Households to Urmia Lake Drying (the Case of Shabestar Region). *Sustainability* **2018**, *10*, 1862. [[CrossRef](#)]
36. Hizbaron, D.R.; Hadmoko, D.S.; Mei, E.T.W.; Murti, S.H.; Laksani, M.R.T.; Tiyansyah, A.F.; Siswanti, E.; Tampubolon, I.E. Towards measurable resilience: Mapping the vulnerability of at-risk community at Kelud Volcano, Indonesia. *Appl. Geogr.* **2018**, *97*, 212–227. [[CrossRef](#)]
37. Bates, P.; Trigg, M.; Neal, J.; Dabrowa, A. *LISFLOOD-FP User Manual*; University of Bristol: Bristol, UK, 2013.
38. Gironás, J.; Roesner, L.A.; Rossman, L.A.; Davis, J. A new applications manual for the Storm Water Management Model(SWMM). *Environ. Model. Softw.* **2010**, *25*, 813–814.
39. Zhu, X.; Dai, Q.; Han, D.; Zhuo, L.; Zhu, S.; Zhang, S. Modeling the high-resolution dynamic exposure to flooding in a city region. *Hydrol. Earth Syst. Sci.* **2019**, *23*, 3353–3372.
40. Tsai, J. *An Agent-Based Computing Method of Urban Vulnerability to Flood Hazard—A Case Study of Liandu, Lishui*; Nanjing Normal University: Nanjing, China, 2019.
41. Programme, U.N.D. *Measuring Human Development: A Primer*; United Nations Development Programme: New York, NY, USA, 2007.
42. Saaty, T.L. A scaling method for priorities in hierarchical structures. *J. Math. Psychol.* **1977**, *15*, 234–281.
43. Kittipongvises, S.; Phetrak, A.; Rattanapun, P.; Brundiens, K.; Buizer, J.L.; Melnick, R. AHP-GIS analysis for flood hazard assessment of the communities nearby the world heritage site on Ayutthaya Island, Thailand. *Int. J. Disaster Risk Reduct.* **2020**, *48*. [[CrossRef](#)]
44. Oh, K.-Y.; Lee, M.-J.; Jeon, S.-W. Development of the Korean Climate Change Vulnerability Assessment Tool (VESTAP)—Centered on Health Vulnerability to Heat Waves. *Sustainability* **2017**, *9*, 1103. [[CrossRef](#)]
45. De Smith, M.J.; Goodchild, M.F.; Longley, P. *Geospatial Analysis: A Comprehensive Guide to Principles, Techniques and Software Tools*; Troubador Publishing Ltd.: Leicester, UK, 2007.

46. Hardy, R.D.; Hauer, M.E. Social vulnerability projections improve sea-level rise risk assessments. *Appl. Geogr.* **2018**, *91*, 10–20. [[CrossRef](#)]
47. Frazier, T.G.; Thompson, C.M.; Dezzani, R.J. A framework for the development of the SERV model: A Spatially Explicit Resilience-Vulnerability model. *Appl. Geogr.* **2014**, *51*, 158–172. [[CrossRef](#)]
48. Armaş, I.; Gavriş, A. Social vulnerability assessment using spatial multi-criteria analysis (SEVI model) and the Social Vulnerability Index (SoVI model)—A case study for Bucharest, Romania. *Nat. Hazards Earth Syst. Sci.* **2013**, *13*, 1481–1499. [[CrossRef](#)]



© 2020 by the authors. Licensee MDPI, Basel, Switzerland. This article is an open access article distributed under the terms and conditions of the Creative Commons Attribution (CC BY) license (<http://creativecommons.org/licenses/by/4.0/>).